Available online at www.sciencedirect.com

ScienceDirect

Procedia Engineering 160 (2016) 53 – 60

Procedia Engineering

www.elsevier.com/locate/procedia

XVIII International Colloquium on Mechanical Fatigue of Metals (ICMFM XVIII)

Fatigue strength assessment of AlSi7Cu0.5Mg T6W castings supported by computed tomography microporosity analysis

C. Garb[a*], M. Leitner[b], F. Grün[c]

[a,b,c]*Montanuniversität Leoben, Department Product Engineering, Chair of Mechanical Engineering, Franz-Josef-Strasse 18, 8700 Leoben, Austria*

Abstract

The fatigue strength of the casted aluminum alloy AlSi7Cu0.5Mg T6W is investigated, whereat different eutectic modifiers, Sr and Na, are used for the two fatigue testing series. The tested specimens are extracted from three different locations of casted cylinder heads. The high-cycle fatigue testing is executed with cylindrical specimens at a load ratio of R = -1. The investigations are supported by CT-scans of the specimens and a comprehensive fractographic analysis. The obtained micro pore sizes from CT-scans are compared with thus of the fractography. It is shown that the maximum micro pore sizes near the surface of both examinations are comparable. The database is statistically evaluated using extremal distribution based functions. To assess the fatigue strength of the imperfected specimen, the simplified crack propagation based approach according to *Tiryakioglu* is applied. The cumulative distribution function matches well to the experimental results. This methodology features the incorporation of extremal micro pore sizes into finite life fatigue strength.

Peer-review under responsibility of the University of Oviedo

Keywords: casted aluminum, fatigue life, micro pore size, CT- scans,

* Corresponding author. Tel.: +43 3842 402-1411; fax: +43 3842 402-1402.
E-mail address: christian.garb@unileoben.ac.at

Peer-review under responsibility of the University of Oviedo
doi:10.1016/j.proeng.2016.08.862

1. Introduction

The automotive industry is continuously tending to improve the efficiency of lightweight drive train components. Especially in highly-stressed fatigue-critical regions, an increasing knowledge of local material properties under working conditions is elementary. One of the most commonly applied materials in lightweight design are aluminum alloys, whereby the microstructure acts as a key influence on the local material properties. Main factors are the micro pore size, dendrite arms spacing (DAS), grain size, oxide films and AlFeSi- phases. Former works [1–5] investigated the dependency of DAS and fatigue life. In addition, numerous researches [6,7] suggest that the DAS as a fatigue factor is insufficient to represent the fatigue strength of the material, rather a correlation between DAS, cooling rate and porosity is more relevant [2]. Herein, the micro pore size and not the porosity as percentage acts as an important influence factor. As long as the micro pore size is larger than other microstructure characteristics it is the determining effect on the fatigue life of aluminum alloys [2,8–10]. For example Wang et al. [3] investigate the influence of casting defects on a A356-T6 aluminum alloy and mentioned the existents of a critical defect size for fatigue crack initiation. For this material the critical defect size is about 25 µm. When the defect size falls below this critical value, the cracks are caused by other initiators, such as slip bands or eutectic particles. Buffiere et al. [10] analyzed the fatigue properties of AlSi7Mg0.3, in connection with casting defects. Micro pores with an equivalent size lower than 50 µm did not lead to crack initiation. In this work, it also distinguished between micro shrinkage and gas pores, which differ mostly in shape. However, the presence of any pores lead to an increase in the possibility of crack initiation. One reason for a higher occurrence of micro pores is based on a modification process of aluminum alloys [11–13]. One of the commonly used modifiers are Strontium (Sr) and Sodium (Na).

The aim of this work is investigate the fatigue strength of the aluminum casting alloy AlSi7Cu0.5Mg T6W by two testing series with different modifiers, Sr and Na. Additional CT-scans of several specimens enable an improved understanding of the micro pore sizes in the different specimen locations. Common distribution functions from literature are applied to the fatigue data to examine potential correlations between the analyzed defect sizes and the fatigue life of the different alloy variations and specimen locations.

2. Experimental

2.1. Material

The utilized specimens were extracted from cylinder heads of an AlSi7Cu0.5Mg aluminum alloy. A T6 heat treatment was performed at all specimens to optimize their mechanical properties. Different modification elements are utilized for the two testing series. For one testing series the aluminum alloy was modified by Sr and for the other Na was used. Both elements are commonly applied as an eutectic modifier in the casting industry today [12]. The silicon morphology in the alloy is modified, which leads to an improvement of the mechanical properties. Side effects of this treatment may be an increasing porosity, which reduces the material strength again [14]. At the beginning of the investigations tensile tests were executed and the DAS of each specimen location from the cylinder heads were determined, see Table 1. The three specimen locations distinguish in the microstructural properties, such as DAS and micro pore sizes.

Table 1. Resulting DAS and ultimate strength

	AlSi7Cu0.5Mg Sr		AlSi7Cu0.5Mg Na	
Position	DAS (µm)	Rm (MPa)	DAS (µm)	Rm (MPa)
1	28	333.9	30	314.8
2	56	317.5	56	228.9
3	67	223.4	60	219.9

2.2. Fatigue tests

The high-cycle fatigue tests were performed with specimens from three different locations within a cylinder head. The specimen locations were selected for the purpose of differences in the microstructure, DAS and micro pore size, and subsequently also variations in static and cyclic material properties. The specimens are cylindrical with a testing diameter of 6 mm and a length of 80 mm. The tests were performed on a resonant testing machine at a load ratio of R = -1 under tension- compression load.

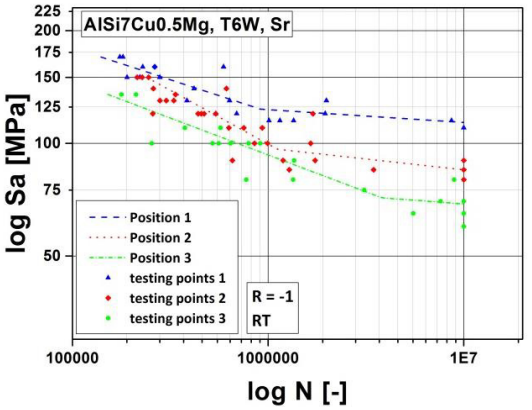

Fig 1. High-cycle fatigue test results for AlSi7Cu0.5Mg Sr

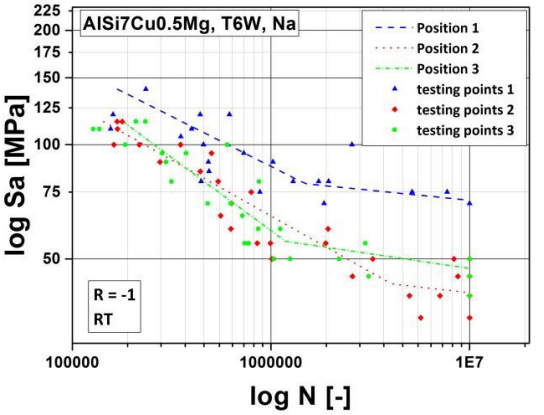

Fig 2. High-cycle fatigue test results for AlSi7Cu0.5Mg Na

The results from the high-cycle fatigue test are shown in Fig 1 and Fig 2 for the different specimen locations and eutectic modifiers. A comparison of the different alloys shows a clear disparity for each specimen location from Sr to Na. The fatigue strength is higher for each location applying the Sr-modified alloy. Generally, the fatigue strength within the testing series decreases from Position 1 to 3, but only for the Na-modified alloy the slope k_1 in the finite life regime of the stress curve is getting smaller from Position 1 to 3. The statistically evaluated results of the SN curves are summarized in Table 2.

Table 2. SN-curve data

	AlSi7Cu0.5Mg Sr			AlSi7Cu0.5Mg Na		
Position	k_1	N_D	$\sigma_{N=10e7}$ (MPa)	k_1	N_D	$\sigma_{N=10e7}$ (MPa)
1	5.85	911,389	113.7	3.80	1,490,740	71.4
2	3.52	1,055,438	86.3	3.39	4,038,166	40.8
3	5.07	3,820,000	68.9	2.60	1,182,288	47.2

2.3. Fractography

For the determination of the failure mechanism, every specimen was fractographically analyzed by SEM. When a micro pore was the cause of failure it`s size was measured. The main crack initiation sources were shrinkage pores (Fig 3), gas pores (Fig 4) and slip planes (Fig 5). Slip planes often occur in presence of micro pores so the failure mechanism may be combined. In general, the crack initiation sources were located near the specimen surface. The results from the evaluated defect sizes are represented in Table 3.

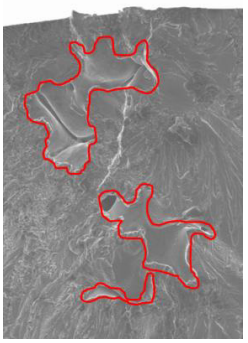

Fig 3. Shrinkage pore

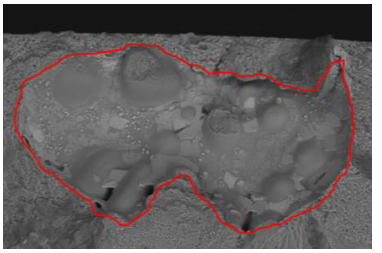

Fig 4. Gas pore

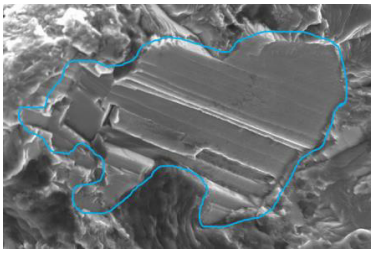

Fig 5. Slip planes

The fatigue test results in combination with the knowledge from the fractography shows that the gas porosity in AlSi7Cu0.5Mg Na is quite high. One reason may be the increased hydrogen content due to the casting process leading to enhanced gas porosity.

2.4. Computed tomography

High resolution computed-tomography analyses were executed on both alloy modifications Sr and Na, see Fig 6. The CT-scans enable the detection of micro pores (Fig 7) in a relative wide size range. To provide a statistically assured evaluation of micro pores in a certain volume, two scan resolutions were defined for the different specimen locations.

Fig 6. CT-scan of high-cycle fatigue specimen

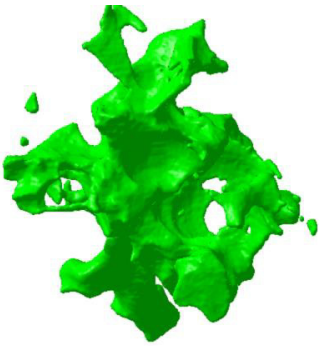

Fig 7. Shrinkage pore

After some test scans, for all specimen locations of AlSi7Cu0.5Mg Sr and Position 1 from AlSi7Cu0.5Mg Na, a resolution of 3 µm voxel size was selected. For Position 2 and 3 of AlSi7Cu0.5Mg Na, the resolution was set to 8 µm voxel size. The possible scan volume for 3 µm voxel size is about 0.2 cm^3 and for 8 µm voxel size about 0.55 cm^3. Five specimens from each position were analyzed by CT. For further investigations the scans enable a detailed analysis of the pore size distribution. In this work, the focus is laid on the largest micro pores per volume. The fractography shows that most of the critical defects appear near the surface. Assessing the micro pore sizes from the CT-scans, at first sight, the evaluated micro pore sizes are significantly larger than the micro pore sizes through fractographic analysis. On contrary extracting only the micro pores near the surface from the CT-scans, the obtained micro pore sizes are within the scatter range of the fractographic results, see Table 3.

Table 3. Micro pore sizes from fractographic analysis and maximum micro pore sizes from CT-scans

	AlSi7Cu0.5Mg Sr			AlSi7Cu0.5Mg Na		
Position	*Fractography (µm)*	*CT whole Volume (µm)*	*CT surface layer (µm)*	*Fractography (µm)*	*CT whole Volume (µm)*	*CT surface layer (µm)*
1	48.8±26.6	132.6±16.1	52.4±30.6	180.0±102.1	335.2±146.4	299.6±143.0
2	72.6±25.1	232.7±23.5	130.3±34.9	352.8±88.0	449.4±114.2	321.7±130.4
3	170.1±46.7	385.4±51.4	307.6±93.3	434.9±136.5	903.4±374.7	648.4±153.3

3. Fatigue life assessment

3.1. Model

The distribution function adopted in this work was developed by Tiryakioglu [15] and combines the size distribution of fatigue-initiating defects with a fatigue life model. Thereby, the distribution of the crack-initiating defects follows a Gumbel distribution [16] as an extreme value distribution, see equation (1). Thereby deq, the equivalent pore diameter, is related to λ and δ, location and scale parameters from the Gumbel distribution. The derivation of the distribution starts with the Paris-Erdogan law [17] and the effective stress intensity factor range.

$$deq = \lambda + \delta \cdot (-\ln(-\ln(P))) \tag{1}$$

Further on, the author derives an equation (2) which combines A_i, the area of the defect on the fracture surface, with the fatigue strength σ_a and lifetime N_f. Herein, the factor m comes from the Paris-Erdogan law and the factor B is introduced by the author.

$$\log(N_f) = \log(B) - m \cdot \log(\sigma_a) + \frac{2-m}{4} \cdot \log(A_i) \tag{2}$$

The derivation leads to a new distribution function (3) from [15], which combines the defect size distribution and fatigue characteristics.

$$P(N_f) = 1 - exp\left(-exp\left(\frac{\lambda}{\delta} - \frac{2}{\delta \cdot \sqrt{\pi}} \cdot \left(\frac{N_f - N_i}{B \cdot {\sigma_a}^{-m}}\right)^{\frac{2}{2-m}}\right)\right) \tag{3}$$

Firstly N_i, the number of cycles to initiate a fatigue crack, can be taken as zero for aluminium casting. This assumption may not be valid in case of a relatively high casting quality leading to comparable small and smoothly shaped defects. In addition, the assumption also loses its validity when the stress level is so low that it takes numerous load cycles to initiate a fatigue crack. However the distribution function is well applicable on the finite life regime.

3.2. Results and Discussion

Two alloy variations from AlSi7Cu0.5Mg modified by Sr and Na, each with three different specimen locations, are compared in regard to fatigue test data and defect sizes. The distribution function from [15] is applied on the data sets. At first, a relation between N_f and A_i (area of the measured defect) cannot be regarded, as seen in Fig 8. It is a first indication if the fatigue life of the data set correlates with the defect size. Subsequently, the parameters for the Gumbel distribution are estimated by the aid of a probability estimator taking the evaluated defect sizes into account. Finally, equation (3) is executed on the data set and the cumulative probability plot is fitted, see Fig 9. For the assessment of the statistical fits a Kolmogorov-Smirnov test (KS-test) [18] is applied on the estimated data.

Although the KS-test is inferior in the estimation of normal distributed data compared to the Anderson-Darling test [19] used by [15], it enables the general testing of the similarity for a data set with a supposed distribution function.

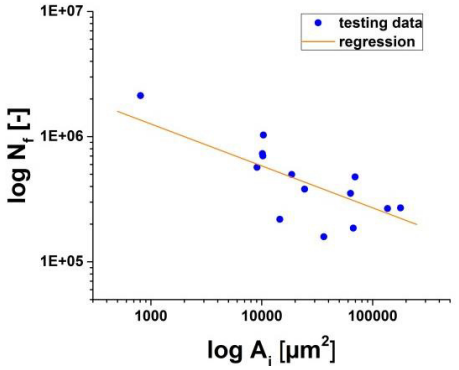

Fig 8. Regression of lifetime N_f against defect area A_i of Position 1 from AlSi7Cu0.5Mg Na

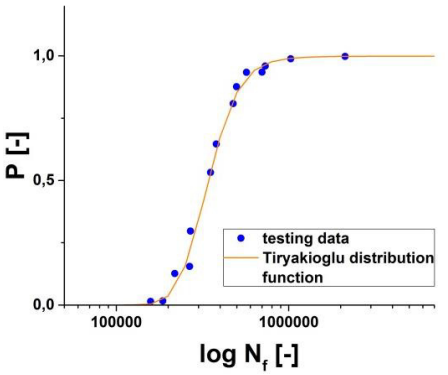

Fig 9. Cumulative probability plot of the Position 1 from AlSi7Cu0.5Mg Na opposed with the testing data

In Table 4 the results of the statistic testing are presented and the valuation parameters, such as the p Value and the test statistic factor, are calculated. The distribution function from [15] and the lognormal distribution are applied on the testing data. The p Value should be above a specific factor, in the literature commonly defined as 0.05 [15], on the contrary, the test statistic factor should tend towards zero. Otherwise, the hypothesis that the data follow the supposed distribution must reject.

Table 4. Results from the Kolmogorov-Smirnov test for the Tiryakioglu distribution and lognormal distribution

	AlSi7Cu0.5Mg Sr				AlSi7Cu0.5Mg Na			
	Tiryakioglu distribution		Lognormal		Tiryakioglu distribution		Lognormal	
Position	Test statistic	p Value	Test statistic	p Value	Test statistic	p Value	Test statistic	p Value
1	0.495	0.025	0.197	0.972	0.379	0.125	0.135	1.000
2	0.354	0.176	0.194	0.978	0.872	0.000	0.253	0.858
3	0.402	0.131	0.282	0.715	0.391	0.066	0.256	0.816

The lognormal distribution is accepted for all investigated data from the KS-test with high p Values. The low test statistic factors suggest an acceptable fitting of the distribution function. The distribution function by Tiryakioglu is only rejecting for two data sets. On the one hand, for Position 1 from the AlSi7Cu0.5Mg Sr, which exhibits comparable small micro pore sizes, and on the other hand, for Position 2 from the AlSi7Cu0.5Mg Na, which is rejecting maybe caused by an undersized specimen lot.

Table 5. Comparison of the fatigue life $N_{50\%}$ on equivalent fatigue stress levels for each specimen location

	AlSi7Cu0.5Mg Sr		AlSi7Cu0.5Mg Na	
Position	*Fatigue test*	Tiryakioglu *distribution*	*Fatigue test*	Tiryakioglu *distribution*
1	392,548	364,428	503,240	383,327
2	651,794	575,344	612,270	464,920
3	1,371,082	1,141,998	462,061	364,036

In common, the Tiryakioglu distribution is slightly less suitable to the testing data, but achieves the requirement to describe the fatigue life distribution. Comparing the expected fatigue life on equivalent fatigue stress levels with the fatigue life of the SN curve by 50 % survival probability, the Tiryakioglu distribution is slightly conservative.

The major benefit by applying this specific distribution is the consideration of the defect size in the fatigue strength assessment of casted Al-alloys.

4. Conclusion

High-cycle fatigue specimen tests, representing the material properties of a cylinder head made of casted aluminum alloy AlSi7Cu0.5Mg T6W were performed. Different eutectic modifiers, Sr and Na, were utilized for the two testing series and in each series three specimen locations from the cylinder head were tested. The fatigue strength of Sr-modified alloy is generally higher than Na-modified alloy for each specimen location. Previous CT-scans of selected specimens were executed to analyze the micro pore size distribution and the occurred maximum pore size. Furthermore, fractographic analysis supported the identification of the failure mechanisms. The micro pore sizes of each specimen location of Sr-modified alloy are lower than those of Na-modified alloy, which is consistent with the distinction in the fatigue strength values. The detected micro pore sizes from the CT-scans concur with those from fractographic analysis, considering only the micro pores near the specimen surface.

Distribution function from Tiryakioglu was applied on the fatigue data sets comparing with lognormal distribution. The evaluation of the statistic fits were conducted with a Kolmogorov-Smirnov test. The lognormal distribution fit is suitable for all data sets, but does not regard the defect size. Except for two specimen locations, the distribution presented by Tiryakioglu describes the testing data sufficiently accurate, due considering the benefit of defect size dependence.

5. Outlook

Future investigations will focus on the crack propagation behavior of the investigated material and a fracture mechanical fatigue strength assessment based on a Kitagawa model [20], which also considers the defect size. Furthermore, comprehensive researches of the micro pore size distributions of specimen with different microstructure will be performed, majorly supported by CT-data.

Acknowledgements

The authors would like to thank Nemak Linz GmbH for the appropriation of the casted components. Further on, execution of the CT scans at the Materials Center Leoben GmbH is highly appreciated. Finally, financial project support was gladly provided by MAGMA Gießereitechnologie GmbH and AVL List GmbH.

Financial support by the Austrian Federal Government (in particular from Bundesministerium für Verkehr, Innovation und Technologie and Bundesministerium für Wissenschaft, Forschung und Wirtschaft) represented by Österreichische Forschungsförderungsgesellschaft mbH and the Styrian and the Tyrolean Provincial Government, represented by Steirische Wirtschaftsförderungsgesellschaft mbH and Standortagentur Tirol, within the framework of the COMET Funding Programme is gratefully acknowledged.

References

[1] Wickberg A, Gustafsson G, Larsson LE. *Microstructural effects on the fatigue properties of a cast A17SiMg alloy*. USA; 1984.
[2] Zhang B, Chen W, Poirier DR. Effect of solidification cooling rate on the fatigue life of A356.2-T6 cast aluminium alloy. *Fatigue & Fracture of Engineering Materials & Structures* 2000;23:417–23.
[3] Wang Q, APELIAN D, Lados D. Fatigue behavior of A356-T6 aluminum cast alloys. Part I. Effect of casting defects. *Journal of Light Metals* 2001;1:73–84, doi:10.1016/S1471-5317(00)00008-0.
[4] Minichmayr R, Eichlseder W. Lebensdauerberechung von Gussbauteilen unter Berücksichtigung des lokalen Dendritenarmabstandes und der Porosität. *Giesserei* 2003;90:70–5.
[5] LADOS D, APELIAN D, DONALD J. Fatigue crack growth mechanisms at the microstructure scale in Al–Si–Mg cast alloys: Mechanisms in the near-threshold regime. *Acta Materialia* 2006;54:1475–86, doi:10.1016/j.actamat.2005.11.019.

[6] Atzori B, Meneghetti G, Susmel L. Fatigue behaviour of AA356-T6 cast aluminium alloy weakened by cracks and notches. *Engineering Fracture Mechanics* 2004;71:759–68, doi:10.1016/S0013-7944(03)00036-5.

[7] Redik S. *Mikrostrukturelle Einflüsse auf das HCF-Ermüdungsverhalten von AlSi- Gusslegierungen*. Dissertation, Montanuniversität Leoben. Leoben; 2014.
[8] Sonsino CM, Dieterich K. Einfluß der Porosität auf das Schwingfestigkeitsverhalten von Aluminium-Gußwerkstoffen - Teil1. *Giessereiforschung 43* 1991:119–30.
[9] Wang Q, APELIAN D, Lados D. Fatigue behavior of A356/357 aluminum cast alloys. Part II – Effect of microstructural constituents. *Journal of Light Metals* 2001;1:85–97, doi:10.1016/S1471-5317(00)00009-2.
[10] Buffière J, Savelli S, Jouneau PH, Maire E, Fougères R. Experimental study of porosity and its relation to fatigue mechanisms of model Al–Si7–Mg0.3 cast Al alloys. *Materials Science and Engineering: A* 2001;316:115–26, doi:10.1016/S0921-5093(01)01225-4.
[11] Haque MM. Effects of strontium on the structure and properties of aluminium-silicon alloys. *Journal of Materials Processing Technology* 1995:193–8.
[12] Hegde S, Prabhu KN. Modification of eutectic silicon in Al–Si alloys. *J Mater Sci* 2008;43:3009–27, doi:10.1007/s10853-008-2505-5.
[13] Campbell J, Tiryakioğlu M. Review of effect of P and Sr on modification and porosity development in Al–Si alloys. *Materials Science and Technology* 2013;26:262–8, doi:10.1179/174328409X425227.
[14] Conley JG, Huang J, Asada J, Akiba K. Modeling the effects of cooling rate, hydrogen content, grain refiner and modifier on microporosity formation in Al A356 alloys. *Materials Science and Engineering: A* 2000;285:49–55, doi:10.1016/S0921-5093(00)00665-1.
[15] Tiryakioğlu M. Relationship between Defect Size and Fatigue Life Distributions in Al-7 Pct Si-Mg Alloy Castings. *Metall and Mat Trans A* 2009;40:1623–30, doi:10.1007/s11661-009-9847-8.
[16] Gumbel EJ. Statistical theory of extreme values and some practical applications: a series of lectures. *Applied mathematics series/ National bereau of standards. U.S. department of commerce (no. 33)* 1954;51 p.
[17] Richard HA, Sander M. *Ermüdungsrisse: Erkennen, sicher beurteilen, vermeiden.* 2nd ed. Wiesbaden: Vieweg+Teubner Verlag; 2012.
[18] Kühlmeyer M. *Statistische Auswertungsmethoden für Ingenieure: Mit Praxisbeispielen*. Berlin: Springer; 2001.
[19] Anderson TW, Darling DA. A Test of Goodness of Fit. *Journal of the American Statistical Association* 1954;49:765–9, doi:10.1080/01621459.1954.10501232.
[20] Kitagawa H, Takahashi S. Applicability of Fracture Mechanics to very small Cracks or the Cracks in the early stage. In: ASM, editor. *Second International Conference on Mechanical Behavior of Materials*; 1976, p. 627–31.